

---

# ENTMOOT: A FRAMEWORK FOR OPTIMIZATION OVER ENSEMBLE TREE MODELS

---

A PREPRINT

**Alexander Thebelt\***  
Imperial College London,  
South Kensington, SW7 2AZ, UK.  
alexander.thebelt18@imperial.ac.uk

**Jan Kronqvist**  
Imperial College London,  
South Kensington, SW7 2AZ, UK.  
j.kronqvist@imperial.ac.uk

**Miten Mistry**  
Imperial College London,  
South Kensington, SW7 2AZ, UK.  
miten.mistry11@imperial.ac.uk

**Robert M. Lee**  
BASF SE,  
Ludwigshafen am Rhein, Germany.  
robert-matthew.lee@basf.com

**Nathan Sudermann-Merx**  
BASF SE,  
Ludwigshafen am Rhein, Germany.  
nathan.sudermann-merx@basf.com

**Ruth Misener**  
Imperial College London,  
South Kensington, SW7 2AZ, UK.  
r.misener@imperial.ac.uk

May 29, 2022

## ABSTRACT

Gradient boosted trees and other regression tree models perform well in a wide range of real-world, industrial applications. These tree models (i) offer insight into important prediction features, (ii) effectively manage sparse data, and (iii) have excellent prediction capabilities. Despite their advantages, they are generally unpopular for decision-making tasks and black-box optimization, which is due to their difficult-to-optimize structure and the lack of a reliable uncertainty measure. ENTMOOT is our new framework for integrating (already trained) tree models into larger optimization problems. The contributions of ENTMOOT include: (i) explicitly introducing a reliable uncertainty measure that is compatible with tree models, (ii) solving the larger optimization problems that incorporate these uncertainty aware tree models, (iii) proving that the solutions are globally optimal, i.e. no better solution exists. In particular, we show how the ENTMOOT approach allows a simple integration of tree models into decision-making and black-box optimization, where it proves as a strong competitor to commonly-used frameworks.

**Keywords** Gradient boosted trees · branch-and-bound · mixed-integer programming · decision-making under uncertainty · black-box optimization

---

\*Corresponding author

## 1 Introduction

Traditional engineering disciplines, e.g. chemical engineering, seek to integrate powerful machine learning tools into their routines and decision-making. Associated industrial applications are often subject to complex systems with high-dimensional input feature spaces. But, while advances in sensor technology led to increased monitoring of industrial manufacturing and large-scale data collection, advanced control equipment often keeps processes close to a few operating states [PR13; Tsa+18]. Manufacturing companies may run experimental studies to maximize data variability and gain system knowledge. However, these experimental studies are often expensive and result in datasets with relatively few datapoints. Coupled with high system dimensionality, this leads to two related challenges: large datasets with low variability and small datasets with high variability.

The models resulting from these datasets pose challenges for classical machine learning methods. The models will be further corrupted by noise, inaccurate measurements and malfunctioning sensor equipment. Therefore, it is inevitable to consider model uncertainty when embedding machine learning models into optimization settings, e.g. larger decision-making. Our proposed approach optimizes over machine learning models in an uncertainty aware setup to prevent excessive extrapolation of such data-driven model architectures. We extend our framework by using the same uncertainty considerations to handle feature space exploration in black-box optimization settings. This way, our tool can (i) guide decision-making when using machine learning models trained with challenging datasets, and (ii) help to improve such datasets by suggesting new promising experimental setups.

Possible data-driven model architectures are Gaussian processes (GPs), artificial neural networks (ANN) and gradient boosted trees (GBTs). Traditionally, GPs automatically account for model uncertainty but may sometimes be limited to smaller datasets with moderate dimension [Sha+16]. ANNs have shown outstanding generalization capabilities for large amounts of data [He+15; Hin+12]. However, ANNs have no built-in model uncertainty measure predicting poor model performance, making them unsuitable for some industrial applications, especially in safety critical environments. Heuristically, GBTs work well in real-world industrial settings [Fri00]. GBTs have many advantages, e.g. (i) handling both numerical and categorical variables, and (ii) robustness against scaling differences in the training data [CG16; Ke+17]. Similar to ANNs, GBTs do not come with a built-in uncertainty measure.

ENTMOOT (**EN**semble **T**ree **MO**del **O**ptimization **T**ool) is an optimization framework that optimizes over pre-trained large-scale GBTs with a built-in uncertainty measure. This measure can either favor solutions in regions with good GBT prediction expectation, or to explore promising areas in the feature space. ENTMOOT derives mathematically proven  $\epsilon$ -global optimal solutions, i.e. no better solutions exist within a pre-determined numerical tolerance. Globally optimal solutions are crucial for decision-making in many industrial applications, e.g. high-throughput production plants where small improvements significantly increase profits, and safety critical applications [BMF16]. For black-box optimization, globally optimal solutions may provide the ideal exploitation and exploration trade-off, given by the acquisition function. Stochastic optimization methods may not find the extreme points of underlying acquisition functions, consisting of complicated surrogate models and uncertainty measures. This is especially true in high dimensions.

## 2 Related Work

When incorporating tree-based models into decision-making and black-box optimization, random forests (RFs) [Bre01] and GBTs [Fri00; Fri02] are popular model architectures. Mišić (2017) first proposed a mixed-integer linear problem (MILP) formulation that integrates RFs into decision-making. Later, Mistry et al. (2018) utilize the same formulation to incorporate GBTs into an optimization setting. Lombardi and Milano (2018) survey embedding machine learning models into large decision-making problems and distinguish several ways of incorporating machine learning models into optimization frameworks. Mistry et al. (2018) and Mišić (2017) rely on traditional optimization techniques to optimize over pre-trained models, while Donti, Amos, and Kolter (2017) train machine learning models to directly output optimal decisions. Donti, Amos, and Kolter (2017) generate decisions (solutions) in close to real time, but lack theoretical guarantees on both constraint satisfaction and obtained solution quality. Traditional optimization-based approaches may be slower, but incorporate rigorous guarantees. ENTMOOT fits into the optimization-based category. ENTMOOT uses the Mišić (2017) formulation for GBTs and combines it with a reliable distance-based model uncertainty measure, making it particularly suitable for decision-making under uncertainty and black-box optimization.

Shahriari et al. (2016) investigate different model architectures for Bayesian optimization (BO). While GPs are generally the most popular choice in BO, there is an ever growing body of research using tree-based models for surrogate model guided black-box optimization. The SMAC framework [HHL11] integrates RFs into BO and proposes a variance estimate for RFs, capturing their model uncertainty in unexplored regions. Similarly, scikit-optimize [The18] utilizes RFs for BO and also offers a framework for using GBTs in black-box optimization. Both SMAC and scikit-optimize rely on stochastic methods for optimizing over surrogate models and cannot give optimality guarantees. ENTMOOT

utilizes deterministic optimization techniques and thereby offers proven  $\epsilon$ -global solutions guaranteed to obey instance specific constraints.

### 3 Proposed Approach

Our main contributions are:

1. We formalize a spatial model uncertainty measure for tree-based ensemble methods quantifying model prediction performance in regions of the input feature space.
2. We propose a mixed-integer nonlinear optimization formulation for optimizing pre-trained tree-based ensemble models incorporating our model uncertainty measure to incentivize optimal solutions close to the training data where accurate model prediction performance is expected. A hyperparameter tunes exploration vs. exploitation. The formulation can incorporate additional constraints representing known relationships between input variables.
3. We present a divide-and-conquer algorithm that effectively optimizes large-scale instances to  $\epsilon$ -global optimality. The algorithm outperforms commercial off-the-shelf optimization software for large tree-based ensemble models with regards to solving time and capability of handling large-scale problems.
4. We introduce a modified mixed-integer nonlinear problem to extend the framework for black-box optimization tasks. Our comprehensive test setup shows that the proposed approach compares well against other black-box optimization toolboxes using tree-based models or GPs.
5. Our approach contributes to data-driven models for optimal decision-making under uncertainty. It is especially attractive in small-data settings or for low observational diversity.
6. Our approach contributes to general machine learning by allowing in-depth analysis of tree-based ensemble models. It determines minimal and maximal model prediction values which helps to understand model behavior and therefore, contributes to its interpretability.
7. The extended framework identifies regions with low data densities that show a high potential for improving the decision-making objective. It compares well against other black-box optimization toolboxes especially in high-dimensional settings and scales well for large datasets.
8. We provide extensive computational studies that show the effectiveness of the proposed model uncertainty measure and the performance of our approach for different random seeds and hyper-parameter settings.

### 4 Spatial Distance as an Uncertainty Measure

GBTs function well as interpolators, i.e. they have good prediction performance when evaluated close to their training data. However, they are poor extrapolators with decreasing prediction performance for unexplored regions of the input feature space not covered by the training data. Large prediction variances w.r.t. the ground truth characterize these unexplored regions. Different methods estimate the model variance of tree-based models, e.g. infinitesimal jackknife and jackknife-after-bootstrap [WHE14; HHL11]. Several software tools use quantile regression [KH01] to quantify uncertainty estimates for both RFs [HHL11; Hut+14], i.e. using quantile regression forests [Mei06], and GBTs [The18]. We propose a different uncertainty estimate  $\alpha(\mathbf{x})$  based on the Euclidean distance squared to the closest point  $\mathbf{x}_d$  in dataset  $\mathcal{D}$  that we define as  $\alpha$ :

$$\alpha(\mathbf{x}) = \min_{d \in \mathcal{D}} \|\mathbf{x} - \mathbf{x}_d\|_2^2. \quad (1)$$

We assume that at locations  $\mathbf{x} \in \mathbb{R}^n$ , where  $n$  defines the dimensionality of the feature space, high values of  $\alpha$  indicate large average model errors. The Euclidean distance squared is a popular measure commonly-used in training algorithms relying on least squares regression to quantify the model error. It is also used in clustering algorithms, e.g. k-means [Llo82], and determines how equal cluster members are to each other.

### 5 Incorporating Tree-Based Models into Decision-Making Problems

In general, decision-making includes optimization problems where we want to determine the extreme points of an underlying model to guarantee that the best option is chosen. When using data-driven models, e.g. GBTs, uncertainty considerations are crucial to determine regions in the input feature space with accurate model predictions. The

optimization problem becomes a trade-off between improving the objective value and regulating model uncertainty. The objective function to this problem is:

$$\min_{\mathbf{x}, \mathbf{z}, \mathbf{y}, \alpha_{pen}} \sum_{t \in \mathcal{T}} \sum_{l \in \mathcal{L}_t} F_{t,l} z_{t,l} + \lambda \alpha_{pen}. \quad (2)$$

We seek to determine  $\mathbf{x}^* \in \mathbb{R}^n$ ,  $\mathbf{z}^*$ ,  $\mathbf{y}^*$  and  $\alpha_{pen}^*$  that minimize Objective (2). The first part of Equation (2) refers to the prediction value returned by the already-trained GBTs, i.e. the sum of leaf value  $F_{t,l}$  parameters. The leaves are indexed by  $t \in \mathcal{T}$  and  $l \in \mathcal{L}_t$ , with  $\mathcal{T}$  and  $\mathcal{L}_t$  defining the set of trees and leaves in every tree  $t$ , respectively. Variables  $z_{t,l} \in \mathbb{R}$  function as binary switches, determining which leaves are active. The continuous variable vector  $\mathbf{x} \in \mathbb{R}^n$  is bounded by the lower bounds  $\mathbf{v}^L$  and upper bounds  $\mathbf{v}^U$  derived from dataset  $\mathcal{D}$ . The second term of the objective function,  $\alpha_{pen}$ , is a variable incentivizing solutions in regions of high data density, where ENTMOOT expects accurate model predictions. We define  $\alpha_{pen}$  in Section 5.1. The tunable parameter  $\lambda$  weights the penalty measure, such that larger values result in more conservative solutions. The objective is subject to the constraints [Miš17]:

$$\sum_{l \in \mathcal{L}_t} z_{t,l} = 1, \quad \forall t \in \mathcal{T}, \quad (3a)$$

$$\sum_{l \in \text{Left}_{t,s}} z_{t,l} \leq y_{i(s),j(s)}, \quad \forall t \in \mathcal{T}, s \in \mathcal{V}_t, \quad (3b)$$

$$\sum_{l \in \text{Right}_{t,s}} z_{t,l} \leq 1 - y_{i(s),j(s)}, \quad \forall t \in \mathcal{T}, s \in \mathcal{V}_t, \quad (3c)$$

$$y_{i,j} \leq y_{i,j+1}, \quad \forall i \in [n], \quad (3d)$$

$$y_{i,j} \in \{0, 1\}, \quad \forall i \in [n], \quad (3e)$$

$$z_{t,l} \geq 0, \quad \forall t \in \mathcal{T}, l \in \mathcal{L}_t. \quad (3f)$$

Equation (3a) ensures that only one leaf per tree contributes to the GBTs prediction. Equations (3b), (3c) and (3d) force all splits  $s \in \mathcal{V}_t$ , leading to an active leaf, to occur in the correct order. Binary switches  $y_{i(s),j(s)}$  determine which splits are active. The continuous variables  $\mathbf{x}$  translate to the intervals  $v_{i,j}$ , defined by the GBTs splits, through linking constraints:

$$x_i \geq v_{i,0} + \sum_{j=1}^{m_i} (v_{i,j} - v_{i,j-1}) (1 - y_{i,j}), \quad (4a)$$

$$\forall i \in [n],$$

$$x_i \leq v_{i,m_i+1} + \sum_{j=1}^{m_i} (v_{i,j} - v_{i,j-1}) y_{i,j}, \quad (4b)$$

$$\forall i \in [n],$$

$$x_i \in [v_i^L, v_i^U], \quad \forall i \in [n]. \quad (4c)$$

## 5.1 Cluster Distance Penalty

A similar uncertainty measure as introduced in Section 4 defines  $\alpha_{pen}$ . To moderate the optimization problem size, we use a clustering algorithm on the training data  $\mathcal{D}$ , e.g. k-means [Llo82], to define a set  $\mathcal{K}$  of clusters. The cluster center positions  $\mathbf{x}_k, \forall k \in \mathcal{K}$  define regions in the input feature space where data is located. This approximates the desired properties of the Section 4 uncertainty measure and defines the variable  $\alpha_{pen}$  in Objective (2), penalizing uncertain regions of feature space  $\mathbf{x}$ . We add the following constraints to the optimization problem:

$$\|\sigma_{diag}^{-1}(\mathbf{x} - \boldsymbol{\mu}) - \mathbf{x}_k\|_2^2 \leq \alpha_{pen} + M(1 - b_k), \quad (5a)$$

$$\forall k \in \mathcal{K},$$

$$\sum_{k \in \mathcal{K}} b_k = 1, \quad (5b)$$

$$\alpha_{pen} \geq 0, \quad (5c)$$

$$b_k \in \{0, 1\}, \quad \forall k \in \mathcal{K}. \quad (5d)$$

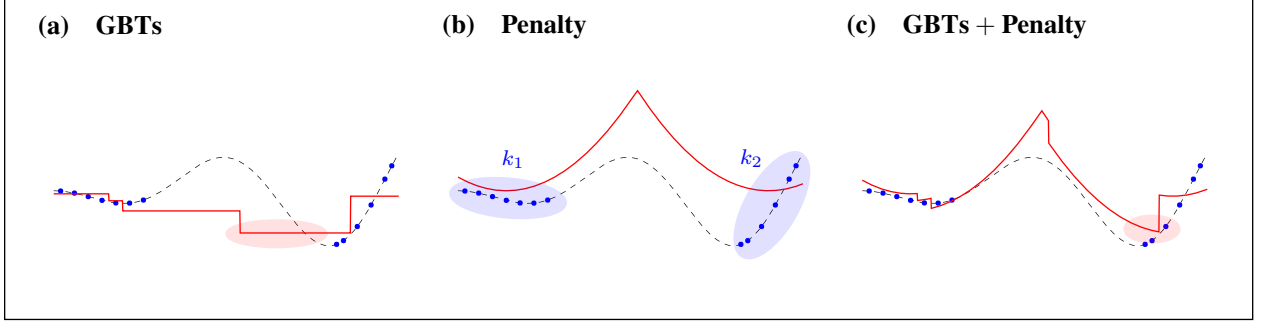


Figure 1: (a) Prediction of  $f(x) = -x \sin(x)$  by GBT model; (b) cluster distance penalty; (c) summation of GBT model prediction and cluster distance penalty.

The clustering algorithm derives the cluster centers from a standardized dataset, requiring the standardization of  $\mathbf{x}$  by the sample mean  $\boldsymbol{\mu}$  and the diagonal matrix  $\boldsymbol{\sigma}_{diag}$ , holding the sample standard deviation, as shown in Equation (5a). So-called “big-M” constraints [NW88] ensure that  $\alpha_{pen}$  takes the value of the Euclidean distance squared to the closest cluster center. Binary variables  $b_k \in \{0, 1\}$  are included into the set of optimization variables and function as a binary switch. When  $b_k = 0$ , the constraint is inactivated and when  $b_k = 1$ , a sufficiently large  $M$  coefficient is multiplied by 0 and effectively disappears. All cluster centers that are inactive have  $b_k = 0$  so that the large value of  $M$  makes their constraints redundant. Equation (5b) enforces exactly one active cluster. The coefficient  $M$  is important, as too large values will result in a weaker problem formulation. Here, the coefficient  $M$  can be calculated:

$$M = \max_{k_1, k_2 \in \mathcal{K}} \|\mathbf{x}_{k_1} - \mathbf{x}_{k_2}\|_2^2 + \max_{k \in \mathcal{K}} r_k, \quad (6)$$

with the left term defining the maximum Euclidean distance squared between two clusters. Radius  $r_k$  is the Euclidean distance squared from the cluster center  $\mathbf{x}_k$  to its most distant cluster member. The optimization model, i.e. Equations (2) – (5), is a convex mixed-integer nonlinear problem (MINLP) [DG86; Kro+19].

## 5.2 Example

To see a simple example of how the penalty influences the optimal solution, we define a system’s ground truth as  $f(x) = -x \sin(x)$ . The function is sampled at 10 positions at the edges of the interval  $[0, 10]$ . Samples in the interval center are purposely avoided to imitate a problematic data collection scenario. We train a simple GBT model using the collected data. However, the sample void in the interval center causes high GBTs prediction errors. As shown in Figure 1 (a), minimizing only the GBT model within ENTMOOT could reveal an optimal point near the undesired maximum value of the ground truth  $f(x)$ . But ENTMOOT seeks to remove model uncertainty with a penalty measure based on data cluster distances. In this simple example, ENTMOOT identifies the two clusters at the edges of the domain of  $f(x)$ . Figure 1 (b) depicts the positive Euclidean distance squared to their cluster centers. Instead of directly minimizing the GBT model, ENTMOOT considers the sum of penalty measure and GBT model prediction. As shown in Figure 1 (c), ENTMOOT effectively shifts the minimum towards the right cluster center and gives a more accurate solution with respect to the ground truth.

## 5.3 Case Study: Fermentation Model

This simple case study uses a mechanistic fermentation model [Zna+04; Elq+13] describing the manufacturing  $C_P$  of a chemical product. Integrating a system of four differential and one algebraic equation determines the production  $C_P$  based on a control sequence  $\mathbf{x}$ . To imitate an industrial sample selection process, we generate the time series input data as blobs using the scikit-learn library [Ped+11]. This sampling strategy evaluates the mechanistic model as a black-box and generates a dataset that is used to train GBTs, utilizing the LightGBM library [Ke+17]. The dimensionality of this problem, i.e. the number of time steps considered for the control sequence, is set to  $\mathbf{x} \in \mathbb{R}^{20}$ , and the dataset consists of 4,000 points. The test setup uses a range of different penalty parameter values and Gurobi 9.0 derives the optimal solution  $\mathbf{x}^*$  of the formulation defined in Section 5 to compute the relative model error depending on penalty parameter  $\lambda$ :

$$\epsilon_{GBT_s}(\lambda) = \frac{GBT_s(\mathbf{x}^*) - BB(\mathbf{x}^*)}{GBT_s(\mathbf{x}^*)} \cdot 100\%, \quad (7)$$

where  $BB(\mathbf{x})$  defines the ground truth of the black-box, obtained from evaluating the fermentation model. Figure 2 depicts the relative model error. The results show a clear trend of decreasing relative model errors  $\epsilon_{GBT_s}(\lambda)$  for high

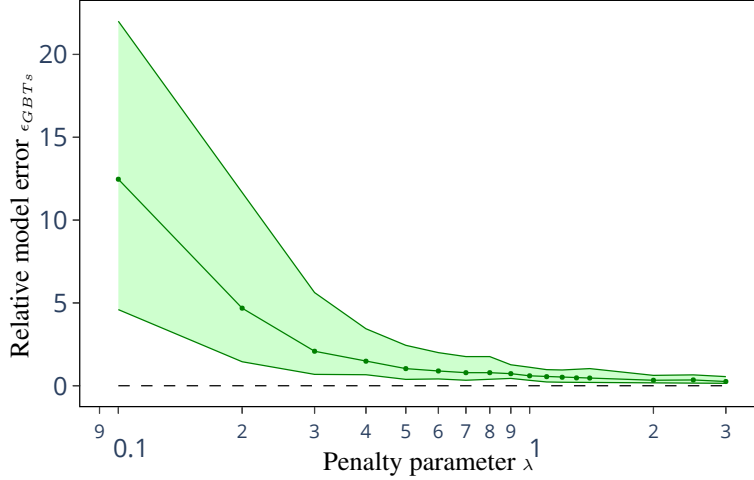


Figure 2: Relative model error  $\epsilon_{GBT_s}$  for different penalty parameters  $\lambda$ . The graph depicts 1<sup>st</sup> quartile, median and 3<sup>rd</sup> quartile based on 50 random seeds.

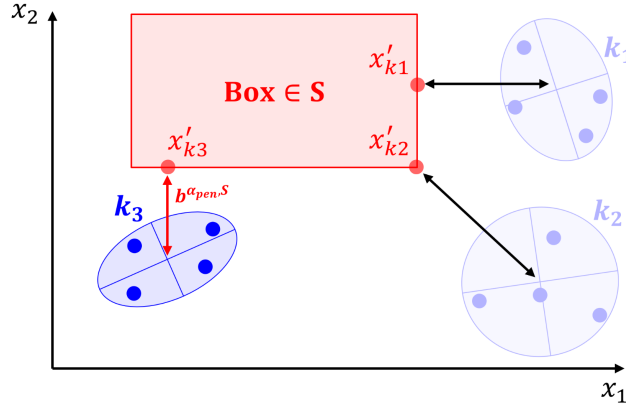


Figure 3: Explicit evaluation of Euclidean distance squared to cluster center projections onto box  $S$  for effective computation of  $b^{\alpha_{pen},S}$ .

penalty parameter values. Large  $\lambda$  values significantly restrict the search domain to a degree that  $x^*$  converges to the cluster center with the lowest objective value. Note in Figure 2, the relative model error converges to a value greater than 0 because there is some model error associated with the cluster center. This error would converge to 0 with more data representing each of the clusters. For reproducibility, Supplementary Material B comprehensively describes the test setup.

### 5.4 Extension for Large Tree Models

When the GBT model becomes extremely large, i.e. more than 2000 trees with a large number of splits per tree, Gurobi 9.0 struggles to prove optimality for the large-scale MINLP. To handle these large-scale instances, ENTMOOT uses a more effective bounding strategy [Mis+18].

Like Gurobi 9.0, ENTMOOT uses a deterministic branch-and-bound approach, divide-and-conquer, over the domain  $[v^L, v^U]$ . Branch-and-bound characterizes every sub-domain in a minimization problem by a lower objective bound on the best possible solution in the domain. Individual domains are rejected for infeasible subproblems or when their lower bound exceeds the current best feasible solution, i.e. the upper bound. Branch-and-bound thereby aims to avoid explicit enumeration of all possible solutions [LD60; Mor+16]. ENTMOOT, like Mistry et al. (2018), uses strong branching to reduce the search space. To compute a new lower bound  $\hat{R}^S$  for domain  $S$ , ENTMOOT decomposes the Objective (2) into two parts:

$$\hat{R}^S = b^{GBTs,S} + b^{\alpha_{pen},S}, \tag{8}$$

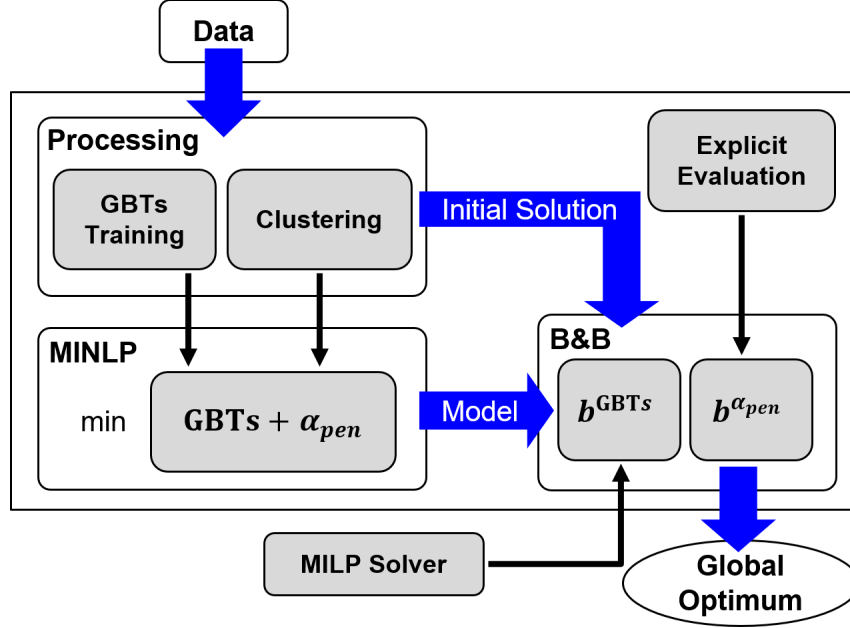


Figure 4: ENTMOOT’s algorithmic setup for large tree models.

where  $b^{\text{GBTs},S}$  and  $b^{\alpha_{pen},S}$  define the objective lower bounds in domain  $S$  for the GBT model and penalty function, respectively. Computing the tightest objective lower bound for  $\text{GBTs}(x)$  in domain  $S$  is NP-hard [Miš17] and hence, difficult to provide for large GBT model instances. ENTMOOT derives a weaker objective lower bound  $b^{\text{GBTs},S}$  by *partition refinement* [Mis+18]. We compute  $b^{\alpha_{pen},S}$  in time linear to the number of clusters multiplied by the number of dimensions, i.e.  $\mathcal{O}(|\mathcal{K}| \cdot n)$ . ENTMOOT does this by calculating the Euclidean distance squared from cluster center  $x_k$  to the projection  $x'_k$  of the cluster center on box  $S$ . ENTMOOT picks the minimum of these distances for  $b^{\alpha_{pen},S}$  or sets it to 0 in case one of the cluster centers is contained in domain  $S$ . Figure 3 depicts this procedure. As  $\alpha_{pen}$  increases for regions distant from training data, deriving a weak bound for  $\text{GBTs}(x)$  can often reject large domains as the “weak” lower bound surpasses the current best feasible solution. For domains not rejected based on this penalty condition,  $b^{\text{GBTs},S}$  is recomputed to derive tighter bounds for  $\text{GBTs}(x)$  in domain  $S$ . After every iteration, the best feasible solution and the lowest lower bound converge and ultimately prove global optimality. In practice, the algorithm terminates after reaching a pre-defined optimality gap between best feasible solution and smallest lower bound. From the structure of the problem, we know that pre-defined cluster centers by definition have  $\alpha_{pen}(x_k) = 0$ . A good initial feasible solution  $x_{feas}$  can therefore be derived by:

$$x_{feas} = \min_{k \in \mathcal{K}} \{\text{GBTs}(x_k)\}. \quad (9)$$

Figure 4 summarizes ENTMOOT’s divide-and-conquer approach for large GBTs.

### 5.5 Case Study: Concrete Mixture

This section tests how better objective lower bounding strategies can help handle large-scale tree models. We utilize the concrete strength dataset [Yeh98] from the UCI machine learning repository [DG17]. The objective is to optimize concrete compressive strength based on ingredient proportions. A GBT model with 4000 trees and a maximum interaction depth of 14 was trained. We compare Gurobi 9 and ENTMOOT runs terminated after a fixed time limit of 4 h and Table 1 shows the bound improvements. ENTMOOT highly benefits from the warm-starting approach and bounding strategy mentioned in Section 5.4 and produces better upper and lower bounds after 4 h of runtime. For blank entries in Table 1, ENTMOOT has proven  $\epsilon$ -global optimality already, with a relative optimality gap of 0.01 %. This happens for large penalty parameter values, as large regions can be rejected quickly. For more details regarding the test setup and more results for different  $\lambda$  values, see Supplementary Material C.

	ENTMOOT		Gurobi 9.0	
$\lambda = 0.1$	ub	lb	ub	lb
1 h	-46.8	-50.8	-40.9	-60.5
2 h	-46.8	-49.1	-43.9	-57.4
3 h	-46.8	-47.8	-45.0	-56.6
4 h	-46.8	-47.6	-45.0	-51.9
$\lambda = 10$	ub	lb	ub	lb
1 h	-46.8	-50.53	-1.1	-60.5
2 h	-46.8	-48.0	-33.6	-57.7
3 h	-	-	-33.6	-56.7
4 h	-	-	-33.6	-56.5

Table 1: Optimization results of ENTMOOT and Gurobi 9.0 for a GBT model that is trained on the concrete mixture design dataset. Blank entries refer to convergence of ENTMOOT with a relative optimality gap of 0.01 %. Notation is: ub: upper objective bound, i.e. best feasible solution found, lb: lower objective bound, i.e. rigorous underestimator.

## 6 Extension for Black-Box Optimization

Black-box optimization computes the input to an unknown system that results in its optimal output, given a pre-defined objective. The unknown system, i.e. the black-box, can be evaluated to get new information about its underlying, unknown function. Black-box optimization algorithms seek to optimize the black-box output, using as few evaluations as possible. Popular approaches include so-called surrogate methods that fit surrogate functions to the data generated from prior black-box evaluations, guiding the optimization. BO is a popular sub-class of these methods and derives surrogate functions from Bayesian statistics [Fra18]. In their BO review, Shahriari et al. (2016) investigate the usage of different surrogate models, e.g. GPs and RFs. The authors highlight the flexibility of RFs to handle various data types, i.e. categorical and conditional variables, scalability for large datasets and good interpolation capabilities. However, Shahriari et al. (2016) point out that the main challenges when using tree-based models remain in proposing consistent model variance estimates for regions of low data density and effective tools to optimize the discontinuous response surface of RFs. SMAC [HHL11] and scikit-optimize [The18] are popular tools incorporating RFs into black-box optimization. The same challenges occur when dealing with GBTs, as their underlying model structure is the same as for RFs. ENTMOOT tackles these challenges by utilizing a consistent uncertainty measure in combination with deterministic global optimization.

### 6.1 Acquisition Function

The acquisition function is the essential part of surrogate methods and is optimized to compute the next most promising black-box evaluation input. It consists of two parts, i.e. exploitation and exploration, trading-off how much each influences the optimization. Exploitation is the guidance given by the surrogate model, i.e. the model is minimized to find the next evaluation input, while exploration defines the incentive to identify promising regions with high model uncertainty still unexplored. A popular acquisition function is the lower confidence bound (LCB) [CJ97]:

$$LCB(\mathbf{x}) = \hat{f}(\mathbf{x}) - \kappa w(\mathbf{x}). \quad (10)$$

In surrogate methods,  $\hat{f}(\mathbf{x})$  and  $w(\mathbf{x})$  describe the surrogate model evaluation and model variance, respectively, at  $\mathbf{x}$ . The parameter  $\kappa$  trades-off exploitation and exploration.

ENTMOOT reformulates the Objective (2) introduced in Section 5 to derive a similar trade-off:

$$\min_{\mathbf{x}, \mathbf{z}, \mathbf{y}, s} \sum_{t \in \mathcal{T}} \sum_{l \in \mathcal{L}_t} F_{t,l,z_t,l} - \kappa \alpha_{expl}. \quad (11)$$

Objective (11) is subject to Constraints (3) and (4). Note that the sign of the right term in Objective (11) has changed compared to Objective (2), incentivizing exploration instead of restricting it.



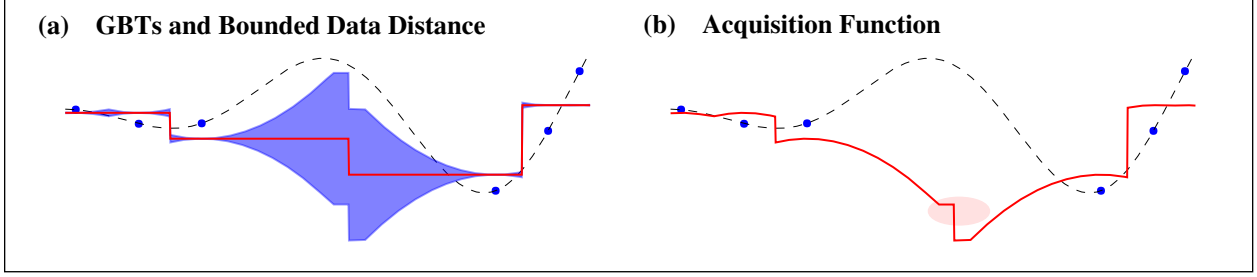


Figure 5: (a) BDD measure for  $f(x) = -x \sin(x)$  GBT model; (b) acquisition function based on BDD measure.

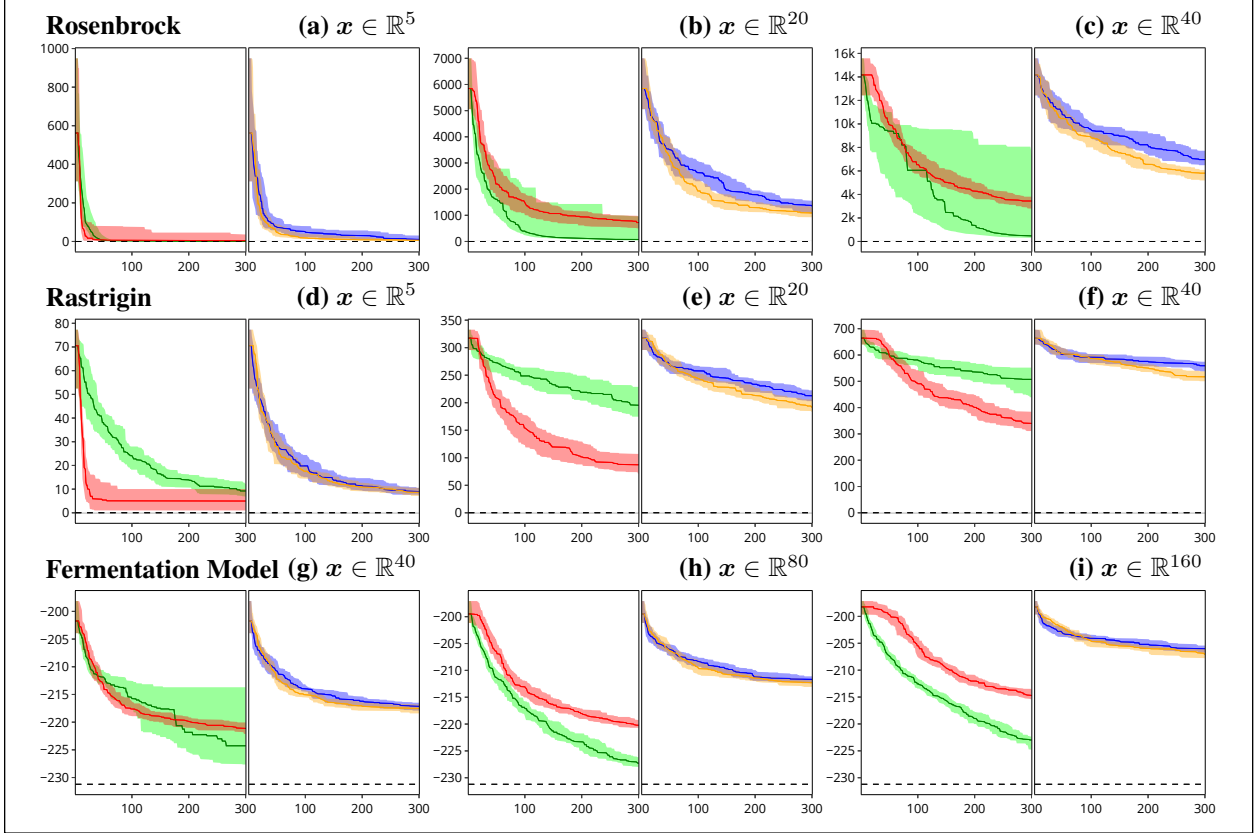


Figure 6: Black-box optimization for different modes (see: Section 7); blue: mode (i), green: mode (ii), orange: mode (iii), red: mode (iv). The graph depicts 1<sup>st</sup> quartile, median and 3<sup>rd</sup> quartile based on 50 random seeds.

## 6.2 Bounded Data Distance Measure

We derive the exploration term  $\alpha_{expl}$  similar to the Section 4 uncertainty measure, considering the Euclidean distance squared to the closest data point of dataset  $\mathcal{D}$ . Constraints (12) define  $\alpha_{expl}$ :

$$\alpha_{expl} \leq \|\sigma_{diag}^{-1}(\mathbf{x} - \boldsymbol{\mu}) - \mathbf{x}_d\|_2^2, \quad (12a)$$

$$\forall d \in \mathcal{D},$$

$$0 \leq \alpha_{expl} \leq \alpha_{limit}. \quad (12b)$$

The big-M constraints are not required, as the sign of the exploration term in Objective (11) is negative now. The minimization pushes  $\alpha_{expl}$  as far away from the nearest data point as possible while the Constraints (12a) to other data points become redundant automatically. As the exploration term  $\alpha_{expl}$  still grows quadratically, we enforce a limit  $\alpha_{limit}$  by introducing Equation (12b), to restrict exploration. The fraction  $\zeta$  of the variance observed in dataset

prediction values  $\mathbf{y}_{\mathcal{D}}$  has shown, in our preliminary studies, to be a good measure:

$$\alpha_{limit} = \zeta \text{Var}(\mathbf{y}_{\mathcal{D}}). \tag{13}$$

Equations (12) and (13) define our bounded data distance (BDD) measure. An intuitive interpretation of bounding the data distance, is that the model uncertainty is bounded. In other words, setting the hyperparameter  $\zeta$  incorporates how much more or less variance we expect compared to what is already evident in dataset  $\mathcal{D}$ . Figure 5 shows the effect of BDD and depicts the resulting acquisition function. Note, while the lack of big-M constraints decrease the number of binary variables, the optimization problem with Objective (11) is a nonconvex MINLP.

## 7 Case Study: Black-Box Optimization

Using the Section 6 formulation, we test our setup on 14 black-box functions, including the Section 5.3 fermentation model and various global optimization test functions [SB20]. To compare our method with existing tools, we use the scikit-optimize library [The18]. For every test, we compare four different modes to evaluate ENTMOOT:

- (i) scikit-optimize: GBTs with variance estimate based on quantile regression, using random evaluation of the acquisition function to minimize it;
- (ii) scikit-optimize: GPs with a radial basis function kernel, using automatic hyperparameter tuning during training, and deactivated noise. A multistart local search is used to minimize the resulting acquisition function;
- (iii) ENTMOOT: GBTs with BDD uncertainty measure (see: Section 6.2), using the same random evaluation points of (i) to minimize the acquisition function;
- (iv) ENTMOOT: GBTs with BDD uncertainty measure, using  $\epsilon$ -global optimization strategy to minimize the acquisition function instead of random sampling.

This setup identifies the effectiveness of the BDD uncertainty measure, i.e. compares (i) and (iii). The setup also shows trade-offs between ENTMOOT and existing approaches, i.e. compares (i), (ii) and (iv). All tests use the LCB acquisition function and start from the same five initial random evaluations of the black-box function. For better comparison, all tests with GBT models, i.e. (i), (iii) and (iv) use the same GBT model training parameters. To achieve better results for mode (ii), the number of multistarts were set to 100 (the default is 5). No further parameters of scikit-optimize are modified. ENTMOOT uses LightGBM (with no hyperparameter tuning) for training the GBT model. For a comprehensive summary of the test setup and additional results, see Supplementary Material D.

Figure 6 shows the results, using the fermentation model, the Rastrigin function and Rosenbrock function as black-box functions. All graphs are based on 50 random states. We report 1<sup>st</sup> quartile, median and 3<sup>rd</sup> quartile for every mode of the best black-box value found at up to 300 iterations. Modes (i) and (iii) perform very similar, indicating that there is no trade-off when using the simple distance-based BDD measure. Approaches relying on random evaluations to optimize the acquisition function, i.e. mode (i) and (iii), perform increasingly poor in higher dimensions. The 10,000 random evaluations are not sufficient for high dimensionality, as the volume of the feature space increases exponentially with the number of dimensions. ENTMOOT compares well against GPs and even outperforms the state-of-the-art method in BO for 46 of the 98 tested instances (see: Supplementary Material D), when considering median performance. However, hyperparameter tuning and testing of different GP variations [Sha+16] might lead to a different performance comparison.

## 8 Discussion and Conclusion

The Section 5.3 penalty parameter study shows that the ENTMOOT penalty measure effectively handles uncertainty in GBT models. A large penalty parameter value relative to the case study (in our instance,  $\lambda > 1$ ) results in relative model errors  $\epsilon_{GBT_s} < 1\%$  for commonly sized GBT models. ENTMOOT thereby directly incorporates GBTs into decision-making, while considering uncertainty. For large datasets, where larger and deeper GBT models are more appropriate, commercial optimization software fails to prove  $\epsilon$ -global optimality. Section 5.4 shows how ENTMOOT scales well for large GBT models by exploiting underlying mathematical structure. The same distance-based uncertainty measure is highly effective when optimizing black-box functions. Section 7 and Supplementary Material D show ENTMOOT as a valuable alternative to commonly used black-box optimization tools. The intuitive BDD measure effectively handles feature space exploration. The  $\epsilon$ -global optimization strategy allows ENTMOOT to perform especially well in high-dimensional settings, where acquisition function optimization via random evaluation is hopeless due to the large feature space dimensionality.

Future research will incorporate the modified optimization problem of Section 6 into the large-scale framework presented in Section 5.4. This allows applying the ENTMOOT approach to large datasets, where the cubic cost of an exact GP

would be high. To increase scalability further, the BDD introduced in Section 6.2 could be approximated by a bounded cluster squared distance, similar to the measure proposed in Section 5.1. One advantage of  $\epsilon$ -global optimization is that it guarantees constraint feasibility to a pre-defined accuracy. This can be exploited when there is additional knowledge about system behavior which is not represented in the collected data. These patterns can be added as constraints to the optimization problem, and ENTMOOT will return  $\epsilon$ -global solutions that satisfy these constraints. This can be useful for decision-making in safety critical applications where satisfying physical constraints is crucial. In black-box optimization, additional constraints can incorporate domain knowledge to guide the underlying data-driven model.

## 9 Acknowledgements

The support of BASF SE, Ludwigshafen am Rhein, the EPSRC Centre for Doctoral Training in High Performance Embedded and Distributed Systems to M.M. (HiPEDS, EP/L016796/1), the Newton International Fellowship by the Royal Society (NIF\R1\182194) to J.K. the grant by the Swedish Cultural Foundation in Finland to J.K. and an EPSRC Research Fellowship to R.M. (EP/P016871/1) is gratefully acknowledged.

## A List of Variables, Parameters, Indices and Sets

Symbol	Definition
$\alpha$	data distance measure
$\mathbf{x}$	feature optimization variables
$\mathbf{z}$	binary variables corresponding to GBTs leaf activity
$\mathbf{y}$	binary variables corresponding to GBTs split activity
$\alpha_{pen}$	binary variables corresponding to GBTs split activity
$\mathbf{v}^L$	vector of lower variable bounds
$\mathbf{v}^U$	vector of upper variable bounds
$\mathbf{b}$	binary variables corresponding to cluster activity
$f$	example function
$\hat{f}$	mean of example function
$C_P$	chemical production, i.e. output of fermentation model
$\epsilon_{GBTs}$	GBT model error percentage
GBTs	output of GBT model
BB	output of black-box function
$\hat{R}$	lower bound of objective
$b^{GBTs}$	lower bound of GBTs part of objective
$b^{\alpha_{pen}}$	lower bound of $\alpha_{pen}$ of objective

Symbol	Definition
$\mathbf{x}'$	projection of $\mathbf{x}$ onto box $S$
$\mathbf{x}_{feas}$	initial feasible solution
$LCB$	lower confidence bound function
$w$	model variance in lower confidence bound
$\alpha_{expl}$	data distance used in ENTMOOT acquisition function
$\alpha_{limit}$	variable upper bound of $\alpha_{expl}$
Var	sample variance
$\mathbf{y}_{\mathcal{D}}$	prediction values of dataset $\mathcal{D}$
$n$	dimensionality of $\mathbf{x}$
$m$	number of variable $x_i$ splitting values
$F$	leaf value
$\lambda$	parameter that weights $\alpha_{pen}$
$\sigma_{diag}$	diagonal matrix with sample standard deviation on its diagonal
$\mu$	sample mean
$M$	Big-M parameter
$r$	cluster radius, i.e. Euclidean squared distance of cluster center to its furthest away cluster member
$\kappa$	parameter that weights $\alpha_{expl}$
$\zeta$	parameter determining $\alpha_{limit}$

Index	Definition
$d$	data point $d \in \mathcal{D}$
$t$	GBT model tree $t \in \mathcal{T}$
$l$	GBT model leaf $l \in \mathcal{L}_t$
*	minimizer of objective function
$i$	vector element $i \in [n]$
$j$	vector element $j \in [m]$
$s$	GBT model split $s \in \mathcal{V}_t$
$k$	cluster $k \in \mathcal{K}$
$S$	box defined by branch-and-bound node

Symbol	Definition
$\mathcal{D}$	set of data points
$\mathcal{T}$	set of GBT model trees
$\mathcal{L}$	set of GBT model leaves
$\mathcal{V}$	set of GBT model splits
Left	set of leaves left to the corresponding split
Right	set of leaves right to the corresponding split
$\mathcal{K}$	set of clusters
$rnd$	set of random seeds

## B Case Study: Fermentation

In this test we seek to show how different penalty parameters  $\lambda$  influence the GBT model uncertainty. This requires knowledge about the ground truth of the underlying system to evaluate the model error. A mechanistic fermentation model [Zna+04; Elq+13] described by a system of differential equations is integrated for different variable settings to generate a dataset. The fermentation model describes how much chemical  $C_P$  is produced based on a control sequence  $\mathbf{x}$ , with  $x \in \mathbb{R}^n$ . The dimensionality  $n$  describes how many discrete timesteps we consider.

To simulate an industrial sample collection procedure we use the blob function from the scikit-learn library [Ped+11]. Based on the feature bounds for  $x_i \in [0, 50]$ , the blob function generates 50 blob centers using a given random seed. The function then generates 4000 samples for  $n = 20$  around these blob centers given a standard deviation of 1.5 in every feature dimension, i.e. every value for  $x_i$  has a standard deviation of 1.5 from the corresponding dimension of the blob center it belongs to. In industrial applications there is often a lot of information at distinct operating points of a system and little information in between. By generating data blobs at different positions in the feature space, we simulate this behavior. These samples are the input to the mechanistic fermentation model and we derive  $C_P$  by integration to derive the dataset. The LightGBM library [Ke+17] trains a GBT model using the parameter specifications in Table 2. Non-specified parameters are at the default values reported by LightGBM.

Penalty parameter values  $\lambda$  are tested in a range from 0 to 1.5 with a step size of 0.1 and three additional values  $\{2, 2.5, 3\}$ . ENTMOOT uses the cluster distance penalty proposed in Section 5.1 and derives its clusters by using k-means [Llo82], implemented in the scikit-learn library. The number of clusters for the k-means algorithm is fixed at 60, making it impossible to accurately spot the blob structure of the generated dataset, consisting of 50 blob centers. Given this setup we minimize the problem defined in Section 5 with Gurobi 9. The two sources of randomness, i.e. generating the sample blobs and training the tree model, are handled by using 50 different random seeds  $rnd \in \{101, 102, 103, \dots, 150\}$ . From all 850 runs, 847 converged to the default relative optimality gap (0.01 %) specified by Gurobi 9, most within a few minutes. For 13 runs, Gurobi 9 struggled to prove  $\epsilon$ -global optimality, and they were terminated after 10 h with a relative optimality gap  $< 6\%$ . Figure 6 summarizes the numerical results by plotting 1<sup>st</sup> and 3<sup>rd</sup> quartile, and the median of runs for different random seeds.

Hyper-parameter	Value
n_trees	200
metric	L2, L1
max_depth	3

Table 2: Hyperparameter selection for GBT model training of the mechanistic fermentation model dataset, using LightGBM.

### C Case Study: Concrete Mixture

Here, we used a publically available dataset [Yeh98] in which describes the compressive strength of concrete, based on its composition and production procedure defined by features  $\mathbf{x} \in \mathbb{R}^8$ . The dataset is available at the UCI machine learning repository [DG17]. We train a large GBT model according to the parameters specified in Table 3. We do not claim that these parameters make sense for this particular test, the point is to show how scalable ENTMOOT is. ENTMOOT uses 500 clusters for the k-means algorithm, determining the clusters for the cluster distance penalty introduced in Section 5.1. When handling such large models, ENTMOOT uses strong branching and partition refinement [Mis+18]. For the strong branching strategy we use a lookahead value of 200, i.e. ENTMOOT evaluates  $b^{\alpha_{pen}, S}$  for the next 200 branches that would be explored and removes them if they lead to lower objective bounds above the best feasible solution found so far. The partition refinement is governed by the initial group size of 20 and a fixed bounding time of 120 s per iteration in ENTMOOT and derives  $b^{\text{GBTs}, S}$ . The underlying MILP solved during partition refinement is handled by Gurobi 9. These hyperparameter specifications were not optimized and are in line with Mistry et al. (2018), where further details regarding the here mentioned algorithmic concepts can be found. Both ENTMOOT and Gurobi 9 were tested for penalty parameter  $\lambda \in \{0.01, 0.1, 1, 10, 100, 1000\}$ , with a time limit of 4 h. Table 4 summarizes the results for all penalty parameter values. Blank entries in Table 4 refer to an early convergence to an  $\epsilon$ -global optimal solution, given a relative optimality gap of 0.01 %. All experiments in Table 4 are run on an Ubuntu 18.04.2 LTS system with 16 GB RAM and an Intel Core i7-7700K @ 4.20 Ghz CPU. For the modeling of the mixed-integer programs and interfacing with solvers, we used Python 3.7.3 in combination with Pyomo 5.6.7 [HWW11; Har+17].

Hyper-parameter	Value
n_trees	4000
metric	L2, L1
max_depth	14
min_data_in_leaf	2
num_leaves	64
random_state	101

Table 3: Hyperparameter selection for GBT model training of the concrete mixture dataset, using LightGBM.

	ENTMOOT		Gurobi 9.0			ENTMOOT		Gurobi 9.0	
$\lambda = 0.01$	ub	lb	ub	lb	$\lambda = 10$	ub	lb	ub	lb
1 h	-46.8	-50.8	-36.5	-60.5	1 h	-46.8	-50.53	-1.1	-60.5
2 h	-46.8	-49.1	-43.9	-57.3	2 h	-46.8	-48.0	-33.6	-57.7
3 h	-46.8	-48.0	-44.1	-56.6	3 h	-	-	-33.6	-56.7
4 h	-46.8	-47.7	-45.8	-56.5	4 h	-	-	-33.6	-56.5
$\lambda = 0.1$	ub	lb	ub	lb	$\lambda = 100$	ub	lb	ub	lb
1 h	-46.8	-50.8	-40.9	-60.5	1 h	-46.8	-49.7	143.9	-60.5
2 h	-46.8	-49.1	-43.9	-57.4	2 h	-	-	143.9	-57.3
3 h	-46.8	-47.8	-45.0	-56.6	3 h	-	-	0.5	-56.5
4 h	-46.8	-47.6	-45.0	-51.9	4 h	-	-	0.5	-51.8
$\lambda = 1$	ub	lb	ub	lb	$\lambda = 1000$	ub	lb	ub	lb
1 h	-46.8	-50.8	-40.9	-60.5	1 h	-46.8	-49.7	143.9	-60.5
2 h	-46.8	-49.1	-43.9	-57.4	2 h	-	-	143.9	-57.3
3 h	-46.8	-47.8	-45.0	-56.6	3 h	-	-	0.5	-56.5
4 h	-46.8	-47.6	-45.0	-51.9	4 h	-	-	0.5	-51.8

Table 4: Optimization results of ENTMOOT and Gurobi 9.0 for a GBT model that is trained on the concrete mixture design dataset. Blank entries refer to convergence of ENTMOOT with a relative optimality gap of 0.01 %. Notation is: ub: upper objective bound, i.e. best feasible solution found, lb: lower objective bound, i.e. rigorous underestimator.

## D Case Study: Black-Box Optimization

To test the black-box optimization extension of ENTMOOT we use the fermentation model (Section 5.3) and several global optimization test functions [SB20], i.e. Rosenbrock, Rastrigin, Sphere, Styblinski-Tang, Ackley, Beale, Booth, Matyas, Schaffer No2, Goldstein-Price, Schaffer No4, 3 Camel Hump and Bukin No6. For functions with variable dimensions, we evaluated  $n \in \{2, 5, 10, 15, 20, 25, 30, 35, 40\}$ . For the fermentation model we used  $n \in \{40, 80, 120, 160\}$ . All other black-box functions are limited to  $n = 2$ . We test four different modes:

- (i) scikit-optimize: GBTs with variance estimate based on quantile regression, using random evaluation of the acquisition function to minimize it;
- (ii) scikit-optimize: GPs with a radial basis function kernel, using automatic hyperparameter tuning during training, and deactivated noise. A multistart local search is used to minimize the resulting acquisition function;
- (iii) ENTMOOT: GBTs with BDD uncertainty measure (see: Section 6.2), using the same random evaluation points of (i) to minimize the acquisition function;
- (iv) ENTMOOT: GBTs with BDD uncertainty measure, using  $\epsilon$ -global optimization strategy to minimize the acquisition function instead of random sampling.

The modes (iii) and (iv) use  $\kappa = 0.1$  and  $\zeta = 0.5$  for all tests, defining the acquisition function in Section 6.1. We consider a total of 300 iterations. Every iteration includes (1) training the surrogate model for each mode based on the current dataset, (2) minimizing the acquisition function consisting of surrogate model and uncertainty measure, (3) evaluating the black-box using the optimizer output and (4) adding the new datapoint to the dataset. Each iteration records the current best value found by each method. For the first five iterations the black-box is evaluated at random inputs to generate an initial dataset, which is the same for all different modes. For better comparison, all modes that use GBTs as surrogate models, use the same set of hyperparameters. We tested two different sets of hyperparameters, i.e. T1 and T2, shown in Table 5. For LightGBM runs we also specified the `metric = L2,L1` and `min_data_in_leaf = 1`. To enhance the performance of mode (ii) we increased the number of multistarts used for minimizing the acquisition function to 100. All other hyperparameters are left at their default values. All graphs show 1<sup>st</sup> and 3<sup>rd</sup> quartile, and the median, based on 50 different random seeds  $rnd \in \{101, 102, 103, \dots, 150\}$ . For mode (iv) we set the Gurobi 9 time limit to 30 min, to moderate the runtime of our tests. However, the majority of Gurobi 9 runs terminated in under 1 min with an  $\epsilon$ -global solution, given a relative optimality gap of 0.01 %. Figures 7, 8, 9, 10, 11 and 12 summarize the results of the 4900 runs.

Hyper-parameter	Value (T1)	Value (T2)
n_trees	500	600
max_depth	3	2

Table 5: Hyperparameter selection for GBT model training of the concrete mixture dataset, using LightGBM.

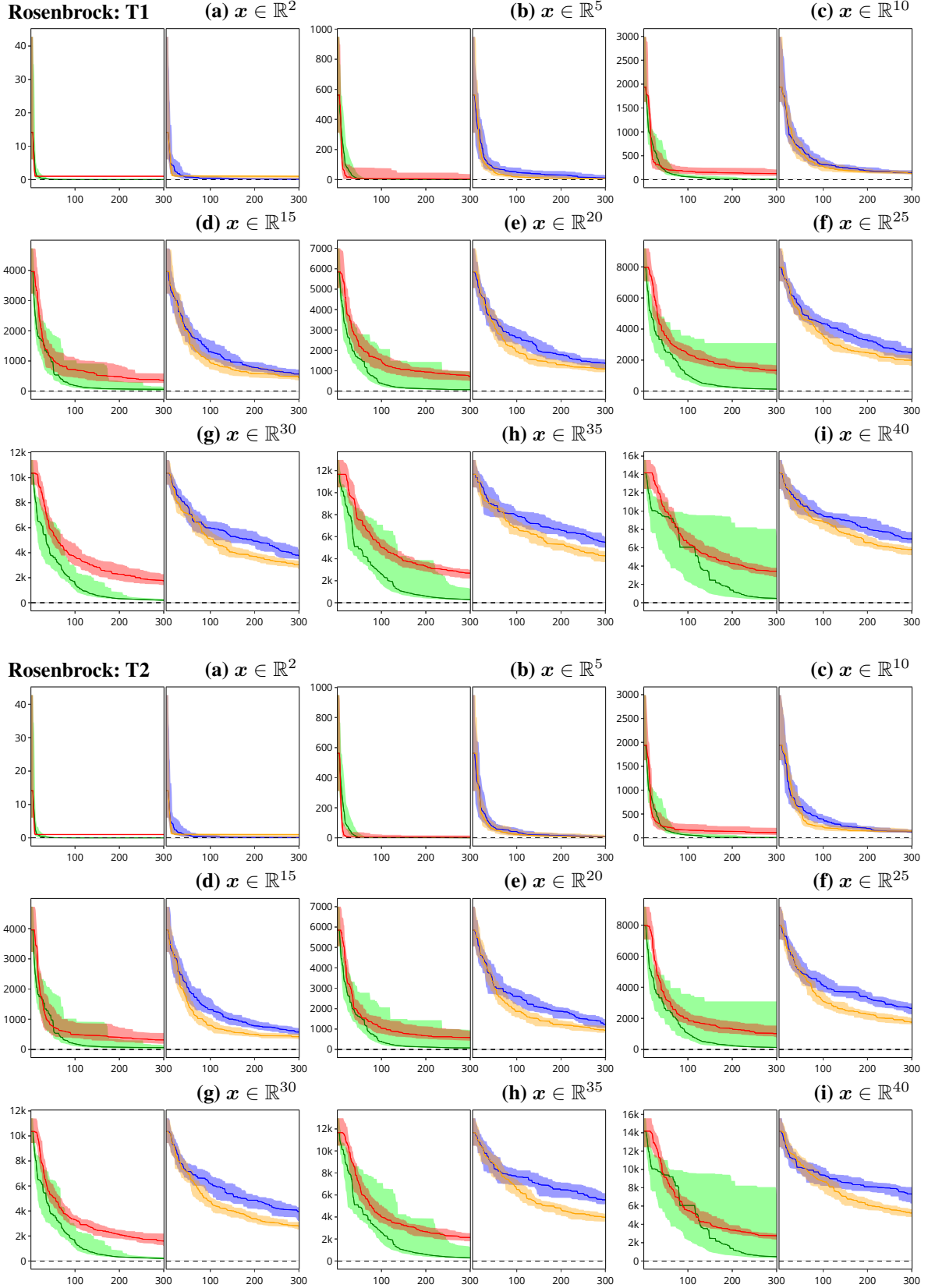


Figure 7: Rosenbrock function, black-box optimization for different GBTs, i.e. T1 and T2 and modes (see: Section D); blue: mode (i), green: mode (ii), orange: mode (iii), red: mode (iv). The graph depicts 1<sup>st</sup> quartile, median and 3<sup>rd</sup> quartile based on 50 random seeds.



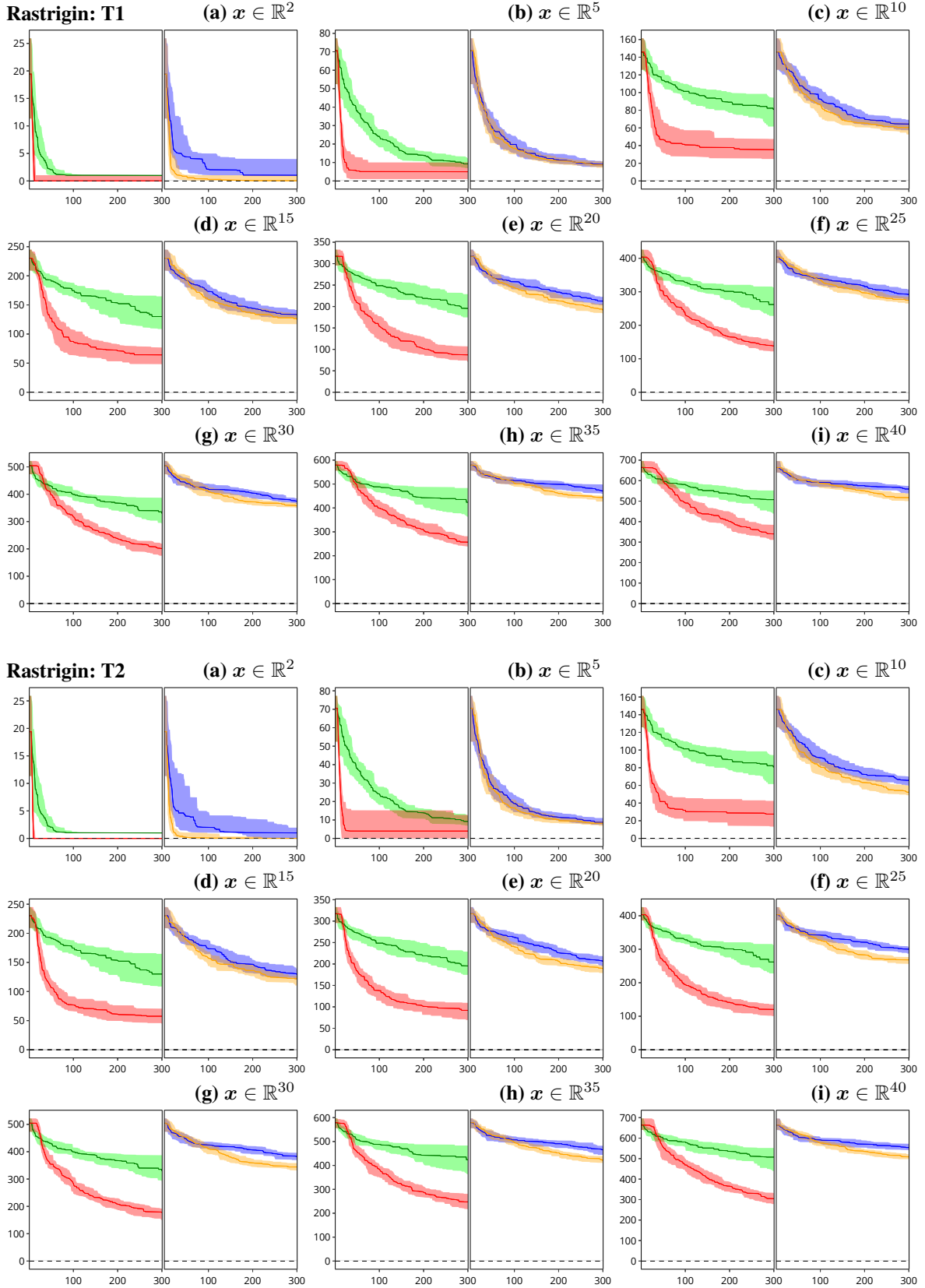


Figure 8: Rastrigin function, black-box optimization for different GBTs, i.e. T1 and T2 and modes (see: Section D); blue: mode (i), green: mode (ii), orange: mode (iii), red: mode (iv). The graph depicts 1<sup>st</sup> quartile, median and 3<sup>rd</sup> quartile based on 50 random seeds.

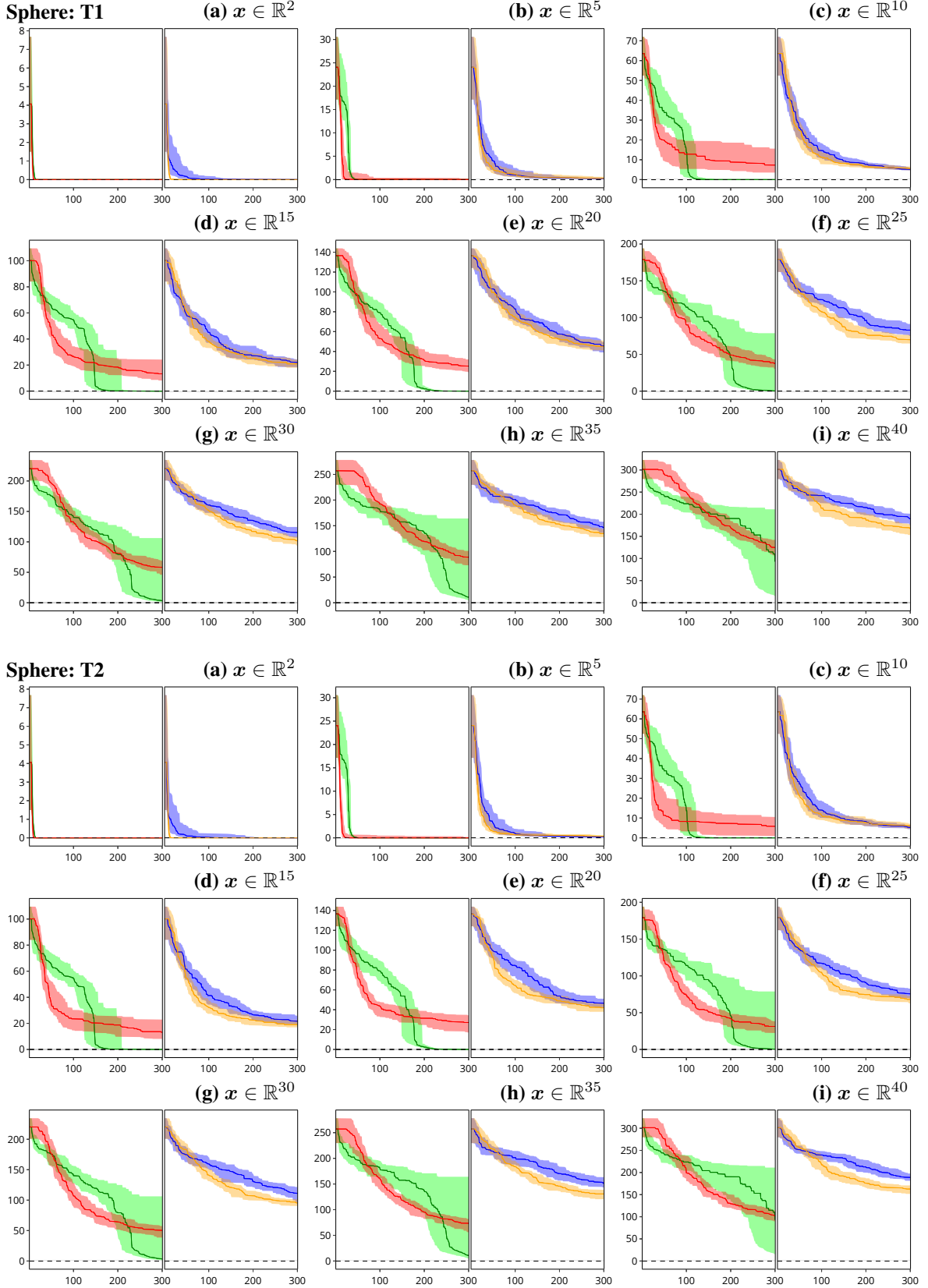


Figure 9: Sphere function, black-box optimization for different GBTs, i.e. T1 and T2 and modes (see: Section D); blue: mode (i), green: mode (ii), orange: mode (iii), red: mode (iv). The graph depicts 1<sup>st</sup> quartile, median and 3<sup>rd</sup> quartile based on 50 random seeds.

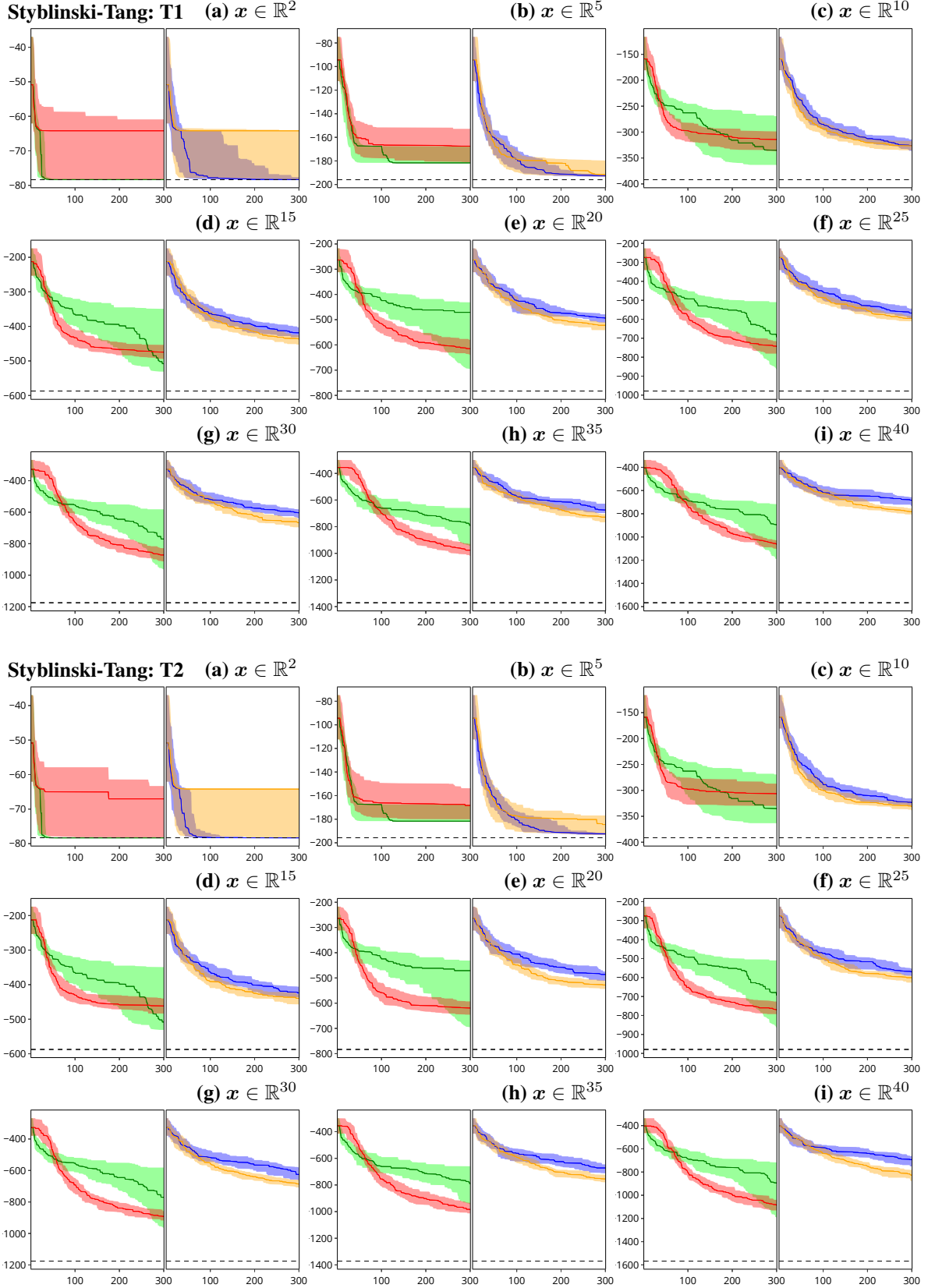


Figure 10: Styblinski-Tang function, black-box optimization for different GBTs, i.e. T1 and T2 and modes (see: Section D); blue: mode (i), green: mode (ii), orange: mode (iii), red: mode (iv). The graph depicts 1<sup>st</sup> quartile, median and 3<sup>rd</sup> quartile based on 50 random seeds.

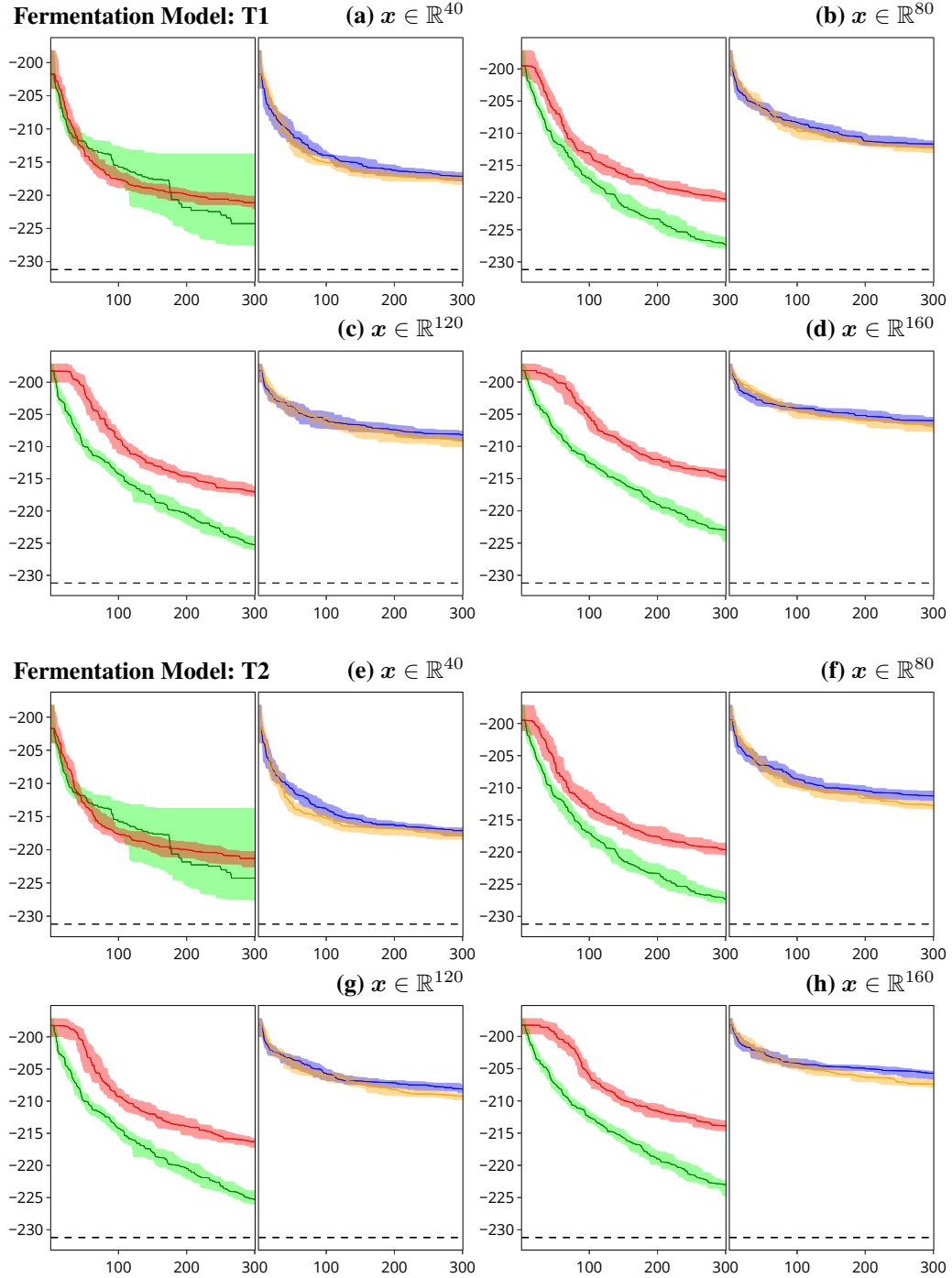


Figure 11: Fermentation model, black-box optimization for different GBTs, i.e. T1 and T2 and modes (see: Section D); blue: mode (i), green: mode (ii), orange: mode (iii), red: mode (iv). The graph depicts 1<sup>st</sup> quartile, median and 3<sup>rd</sup> quartile based on 50 random seeds.

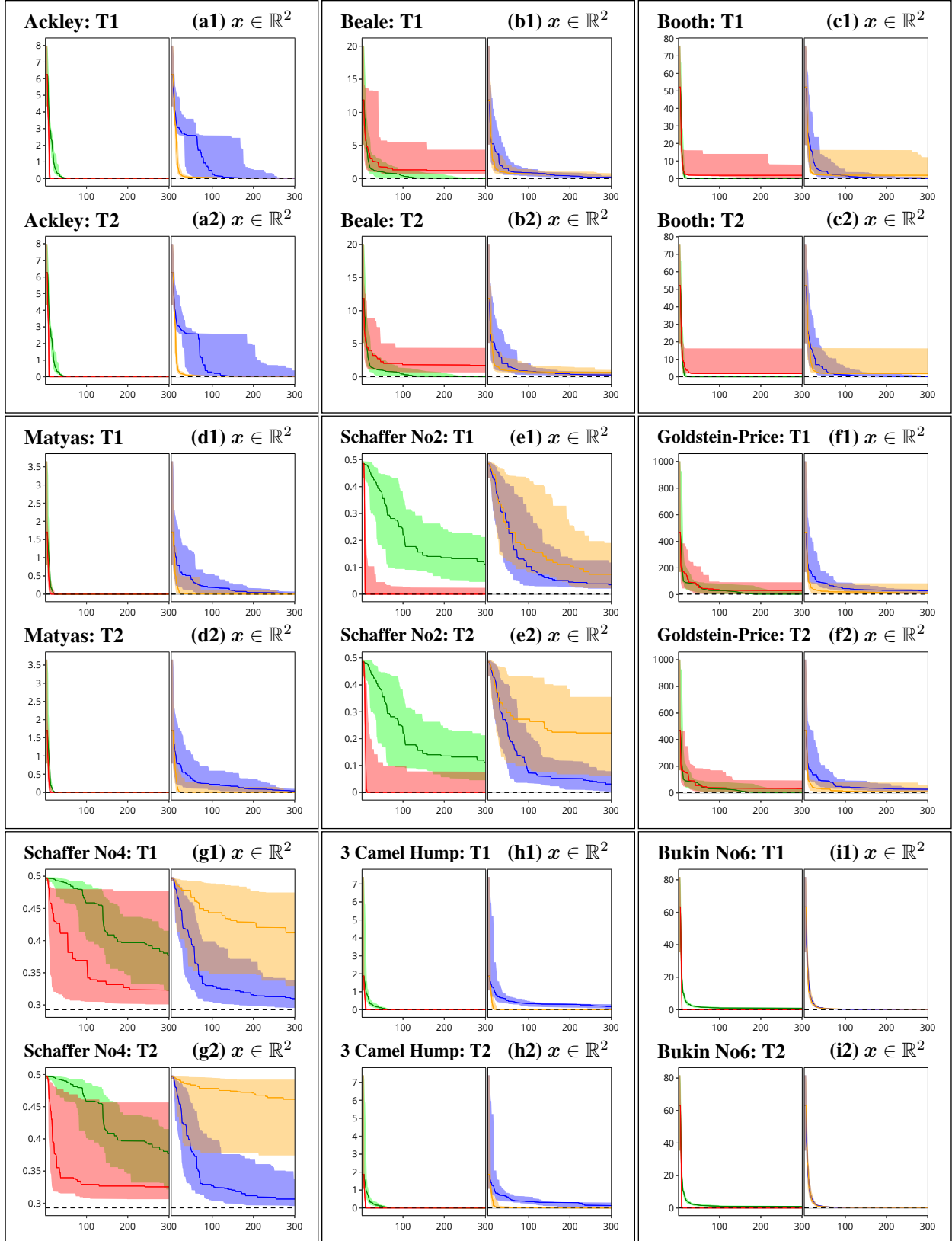


Figure 12: 2D functions, black-box optimization for different GBTs, i.e. T1 and T2 and modes (see: Section D); blue: mode (i), green: mode (ii), orange: mode (iii), red: mode (iv). The graph depicts 1<sup>st</sup> quartile, median and 3<sup>rd</sup> quartile based on 50 random seeds.

## References

- [BMF16] Fani Boukouvala, Ruth Misener, and Christodoulos A. Floudas. “Global optimization advances in Mixed-Integer Nonlinear Programming, MINLP, and Constrained Derivative-Free Optimization, CDFO”. In: *European Journal of Operational Research* 252.3 (2016), pp. 701–727.
- [Bre01] Leo Breiman. “Random Forests”. In: *Machine learning* 45.1 (2001), pp. 5–32.
- [CG16] Tianqi Chen and Carlos Guestrin. “XGBoost: A Scalable Tree Boosting System”. In: *Proceedings of the 22nd ACM SIGKDD International Conference on Knowledge Discovery and Data Mining*. KDD ’16. San Francisco, California, USA: Association for Computing Machinery, 2016, pp. 785–794.
- [CJ97] Dennis D. Cox and Susan John. “SDO: A Statistical Method for Global Optimization”. In: *Multidisciplinary Design Optimization: State of the Art*. Society for Industrial & Applied Mathematics, 1997, pp. 315–329.
- [DAK17] Priya L. Donti, Brandon Amos, and J. Zico Kolter. “Task-Based End-to-End Model Learning in Stochastic Optimization”. In: *Proceedings of the 31st International Conference on Neural Information Processing Systems*. NIPS’17. Long Beach, California, USA: Curran Associates Inc., 2017, pp. 5490–5500.
- [DG17] Dheeru Dua and Casey Graff. *UCI Machine Learning Repository*. 2017. URL: <http://archive.ics.uci.edu/ml>.
- [DG86] M. A. Duran and I. E. Grossmann. “An outer-approximation algorithm for a class of mixed-integer nonlinear programs”. In: *Mathematical Programming* 36.3 (1986), pp. 307–339.
- [Elq+13] M. Elqotbi et al. “CFD modelling of two-phase stirred bioreaction systems by segregated solution of the Euler-Euler model”. In: *Computers & Chemical Engineering* 48 (2013), pp. 113–120.
- [Fra18] Peter I. Frazier. “A Tutorial on Bayesian Optimization”. In: *ArXiv* 1807.02811 (2018).
- [Fri00] Jerome H. Friedman. “Greedy Function Approximation: A Gradient Boosting Machine”. In: *Annals of Statistics* 29 (2000), pp. 1189–1232.
- [Fri02] Jerome H Friedman. “Stochastic gradient boosting”. In: *Computational statistics & data analysis* 38.4 (2002), pp. 367–378.
- [Har+17] William E Hart et al. *Pyomo — Optimization Modeling in Python*. Vol. 67. Springer Optimization and Its Applications. Springer International Publishing, 2017.
- [He+15] Kaiming He et al. “Delving Deep into Rectifiers: Surpassing Human-Level Performance on ImageNet Classification”. In: *2015 IEEE International Conference on Computer Vision*. ICCV. 2015, pp. 1026–1034.
- [HHL11] Frank Hutter, Holger H. Hoos, and Kevin Leyton-Brown. “Sequential Model-Based Optimization for General Algorithm Configuration”. In: *Proceedings of the 5th International Conference on Learning and Intelligent Optimization*. LION’05. Rome, Italy: Springer-Verlag, 2011, pp. 507–523.
- [Hin+12] Geoffrey Hinton et al. “Deep Neural Networks for Acoustic Modeling in Speech Recognition: The Shared Views of Four Research Groups”. In: *IEEE Signal Processing Magazine* 29.6 (2012), pp. 82–97.
- [Hut+14] Frank Hutter et al. “Algorithm Runtime Prediction: Methods & Evaluation”. In: *Artificial Intelligence* 206 (2014), pp. 79–111.
- [HWW11] William E Hart, Jean-Paul Watson, and David L Woodruff. “Pyomo: modeling and solving mathematical programs in Python”. In: *Mathematical Programming Computation* 3.3 (2011), pp. 219–260.
- [Ke+17] Guolin Ke et al. “LightGBM: A Highly Efficient Gradient Boosting Decision Tree”. In: *Proceedings of the 31st International Conference on Neural Information Processing Systems*. NIPS’17. Long Beach, California, USA: Curran Associates Inc., 2017, pp. 3149–3157.
- [KH01] Roger Koenker and Kevin F. Hallock. “Quantile Regression”. In: *Journal of Economic Perspectives* 15.4 (2001), pp. 143–156.
- [Kro+19] Jan Kronqvist et al. “A review and comparison of solvers for convex MINLP”. In: *Optimization and Engineering* 20.2 (2019), pp. 397–455.
- [LD60] A. H. Land and A. G. Doig. “An automatic method of solving discrete programming problems”. In: *Econometrica* 28 (1960), pp. 497–520.
- [Llo82] Stuart P. Lloyd. “Least Squares Quantization in PCM”. In: *IEEE Transactions on Information Theory* 28.2 (1982), pp. 129–137.
- [LM18] Michele Lombardi and Michela Milano. “Boosting combinatorial problem modeling with machine learning”. In: *IJCAI International Joint Conference on Artificial Intelligence*. International Joint Conferences on Artificial Intelligence, 2018, pp. 5472–5478.
- [Mei06] Nicolai Meinshausen. “Quantile Regression Forests”. In: *Journal of Machine Learning Research* 7 (2006), pp. 983–999.

- [Mis+18] Miten Mistry et al. “Mixed-Integer Convex Nonlinear Optimization with Gradient-Boosted Trees Embedded”. In: *ArXiv* 1803.00952 (2018).
- [Miš17] Velibor V Mišić. “Optimization of Tree Ensembles”. In: *ArXiv* 1705.10883 (2017).
- [Mor+16] David R. Morrison et al. “Branch-and-bound algorithms: A survey of recent advances in searching, branching, and pruning”. In: *Discrete Optimization* 19 (2016), pp. 79–102.
- [NW88] George Nemhauser and Laurence Wolsey. *Integer and Combinatorial Optimization*. Hoboken, NJ, USA: John Wiley & Sons, Inc., 1988.
- [Ped+11] Fabian Pedregosa et al. “Scikit-learn: Machine learning in Python”. In: *Journal of Machine Learning Research* 12 (2011), pp. 2825–2830.
- [PR13] Constantinos C. Pantelides and J. G. Renfro. “The online use of first-principles models in process operations: Review, current status and future needs”. In: *Computers & Chemical Engineering* 51 (2013), pp. 136–148.
- [SB20] S. Surjanovic and D. Bingham. *Virtual Library of Simulation Experiments: Test Functions and Datasets*. 2020. URL: <http://www.sfu.ca/~ssurjano>.
- [Sha+16] Bobak Shahriari et al. “Taking the Human Out of the Loop: A Review of Bayesian Optimization”. In: *Proceedings of the IEEE* 104.1 (2016), pp. 148–175.
- [The18] The scikit-optimize contributors. *scikit-optimize/scikit-optimize: v0.5.2*. Version v0.5.2. 2018. URL: <https://doi.org/10.5281/zenodo.1207017>.
- [Tsa+18] Calvin Tsay et al. “A survey of optimal process design capabilities and practices in the chemical and petrochemical industries”. In: *Computers & Chemical Engineering* 112 (2018), pp. 180–189.
- [WHE14] Stefan Wager, Trevor Hastie, and Bradley Efron. “Confidence Intervals for Random Forests: The Jackknife and the Infinitesimal Jackknife”. In: *Journal of Machine Learning Research* 15 (2014), pp. 1625–1651.
- [Yeh98] I. C. Yeh. “Modeling of strength of high-performance concrete using artificial neural networks”. In: *Cement and Concrete Research* 28.12 (1998), pp. 1797–1808.
- [Zna+04] H Znad et al. “A kinetic model for gluconic acid production by *Aspergillus niger*”. In: *Chemical Papers* 58.1 (2004), p. 23.